

# Self-organized, supercritical shock waves in granular matter under swirling excitation

Song-Chuan Zhao

*Institute for Multiscale Simulation, Friedrich-Alexander-Universität,*

*Cauerstraße 3, 91058 Erlangen, Germany and*

*State Key Laboratory for Strength and Vibration of Mechanical Structures,*

*School of Aerospace Engineering, Xi'an Jiaotong University, Xi'an 710049, China*

Thorsten Pöschel

*Institute for Multiscale Simulation, Friedrich-Alexander-Universität,*

*Cauerstraße 3, 91058 Erlangen, Germany*

## Abstract

We study here the spontaneous clustering of a submonolayer of grains under horizontal circular shaking. The clustering of grains occurs when increasing the oscillation amplitude beyond a threshold. The dense area travels in a circular fashion at the driving frequency, even exceeds the velocity of the driving. It turns out that the observed clustering is due to the formation of density wave. The velocity of individual grains increases with the local density, a manifestation of multiplicative driving. The analysis of a phenomenological model shows that the instability of the uniform density profile arises by increasing the oscillation amplitude and captures the non-monotonic dependence of the transition amplitude of the clustering on the global density of the system. The interplay of dissipative particle-particle interaction and the frictional driving of the substrate results into the multiplicative driving, which is tested with DEM Simulations.

Owing to its non-equilibrium nature, granular materials exhibit phenomena of self-organization across orders of magnitude, from gold panning [15] to astrophysics [16, 17]. Those phenomena are largely represented by the clustering instability, non-uniform density distribution developing out of an initially homogeneous state. Clustering has been observed both in freely cooling granular gas [18] and in driven systems [19]. Such a collective behavior leads to pattern formation [20], segregation [15, 21] and phase separation [17]. Though clustering of granular matter exhibits some generic features across various systems, there are peculiarities in any particular system that need to be taken into account, *e.g.*, the type of energy input [22]. Unraveling the physics mechanism represents a crossroad of hydrodynamics, nonequilibrium statistical mechanics and the phenomenological theory of pattern formation, which has attracted interest over decades. The discovery of new features challenges the existing concepts and theories [23]. One may refer to Refs 17 and 24 and references therein for an overview. In this article, we study a submonolayer of beads under horizontal agitations. The constant frictional driving of the substrate distinguishes it from vertically vibrated systems. Strip-like patterns were reported in such systems subjected to a one-dimensional oscillation [20]. Under two-dimensional oscillation, a liquid-solid transition was found, and the solid phase is reached by increasing the oscillation amplitude [21], an example of ‘freezing by heating’. However, the mechanism of the spontaneous clustering in such a system is still unknown. Here, we untangle this issue by combining experiments, a phenomenological model and DEM Simulations.

For the system studied here, there are three important experimental parameters: the oscillation strength, the global packing density and the ratio of the grain size to the container size. We first study a reference system specified and later we investigate the influence of various parameters to the system behavior. The submonolayer consists of  $N_{tot} = 6,930$  polydisperse ceramic beads of diameter  $[0.6 \dots 0.8]$  mm with uniform distribution and the mean  $d_g = 0.7$ mm. The grains located on the bottom plate are confined by a circular side wall of diameter  $D = 82$ mm. The global packing density is given by the area ratio  $\phi_{tot} = N_{tot}(d_g/D)^2$ . The inclination of the bottom plate is smaller than 0.02 mm/m. The container is subjected to anti-clockwise circular oscillation in the horizontal plane of frequency 5 Hz. The oscillation amplitude is varied in the range  $A = [5 \dots 13]$ mm. Note that here the amplitude represents the diameter of the circular oscillation path [cf. Fig. 1b]. In this range of agitation, grains rarely jump over each other and, thus, the packing remains two-

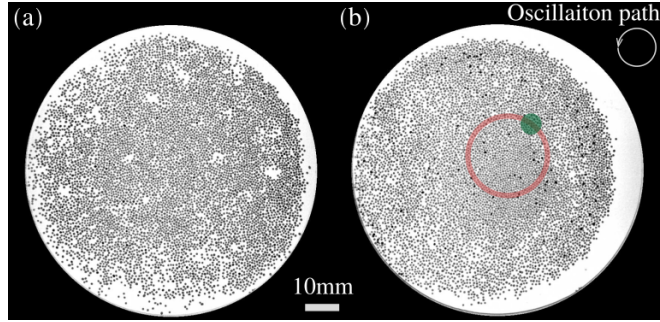


FIG. 1. Snapshots of the packing for two oscillation amplitudes: (a)  $A = 5\text{mm}$  and (b)  $A = 11\text{mm}$ . A dense area can be seen at the center for (b). In (b) the red circle indicates a stationary path of diameter  $22\pi\text{mm}$  in the lab frame of reference, along which the local density profile in Fig. 2a is computed. See the main text for more information. The green solid circle indicates the typical region where individual grains would access during one oscillation cycle. The white circle indicates the anti-clockwise oscillation path in scale.

dimensional. The system is illuminated by a LED panel from the bottom, and the dynamics are captured by a high speed camera (Mikrotron MC1362) at the top. The camera is fixed in the laboratory frame of reference. In the following, the analysis is done in this frame for reference.

Figure 1 shows snapshots of the system at two oscillation amplitudes. For  $A = 5\text{mm}$ , the system is homogeneous. For  $A = 11\text{mm}$ , a cluster of grains can be seen at the center. The observed clustering is very sensitive to the oscillation amplitude. The dense area disappears within 10 cycles after decreasing  $A$  from  $11\text{mm}$  to  $10\text{mm}$ . The transition is thus reversible. This highlights the uniqueness of the clustering in the current work with respect to that in a vertically vibrated monolayer [25]. There, hysteresis is observed in the clustering transition. Furthermore, in our experiments the dense area moves anti-clockwise, the same direction as the oscillation [see SI movies].

In Fig. 1b there are dense areas at the right periphery of the packing. Those dense boundary layers may be sustained over many cycles and move in a counter-intuitive way, opposite to the swirling motion. Nevertheless, the occurrence of a dense area near the periphery is not surprising. The rotational degree of freedom of grains reduces the linear momentum transfer from the substrate [26]. Therefore, grains move slower than the container, and there is an apparent velocity gradient between the grains and the side wall. In consequence, those

grains at the periphery of the packing are condensed during certain oscillation phases by the fast moving side wall. In contrast, the spontaneous clustering at the center of the packing can not be explained by this argument. To understand the mechanism of the clustering we study the dynamics of the particles. To avoid the potential influence of the boundary layers, we exclude particles closer than  $15d_g$  to the side wall from the analysis.

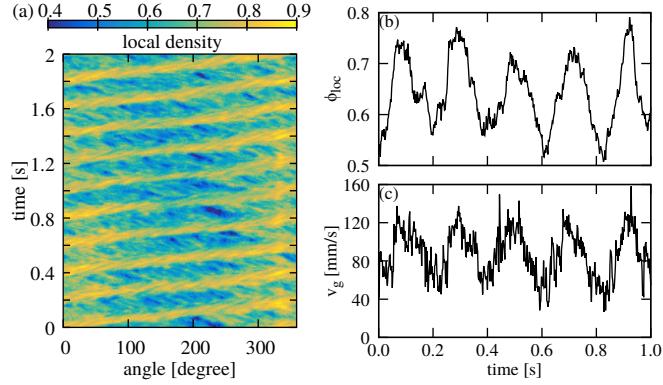


FIG. 2. (a) Local density profile along a circular path versus time for  $A = 11\text{mm}$  and  $N_{tot} = 6930$ , where clustering at the center is observed. The circular path used here is highlighted in red in Fig. 1b. The exact position of the path is given in the main text. (b) For the same experiment, the local density  $\phi_{loc}$  and the velocity of a grain  $v_g$  on the circular path display positive correlations. See main text for the definition of  $\phi_{loc}$ .

To visualize the motion of the dense area, we select a circular path in the lab frame and calculate the local density profile along this path. The path is concentric with the moving line of the center of the bottom plate, but has a larger diameter of 22 mm. The local density  $\phi_{loc}$  is defined for individual grains in a circular neighborhood with a diameter of  $5d_g$ . The upper bound of  $\phi_{loc}$  is  $\phi^* \approx 0.9$  corresponding to the hexagonal packing.  $\phi_{loc}$  along this circular path is plotted versus time in Fig. 2a. It is noticeable that the maximum of  $\phi_{loc}$  travels at the same frequency as the driving (5 Hz), while covering a distance of  $22\pi$  mm during one cycle, twice the swirling motion of the container  $\pi A = 11\pi\text{mm}$ . In other words, the motion of  $\phi_{loc}$  is faster than the oscillation itself. As explained above, due to the rotational degree of freedom, the grains move slower than the oscillation. This implies that the observed motion is the propagation of density waves.

Meanwhile the trajectory of individual grains is still confined to a region much smaller than the size of the oscillation path. For comparison, the region in which a grain on the

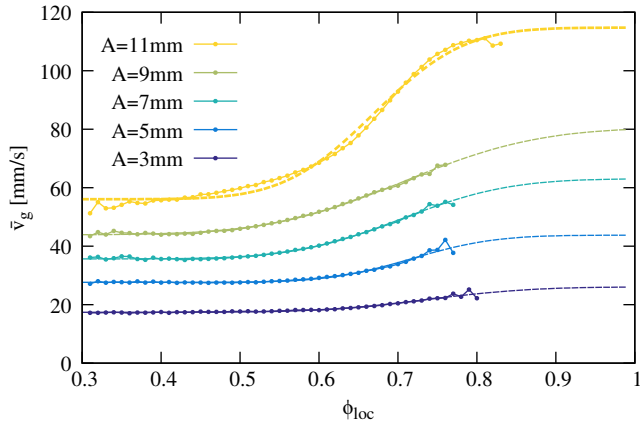


FIG. 3. The presumed value of the velocity of grains,  $\bar{v}_g$ , increases with the local density,  $\phi_{loc}$ , for various oscillation amplitude  $A$ .  $A = 11\text{mm}$  triggers the clustering/density wave at the center of the packing. The dashed lines are fits of the error function to the data.

circular path moves during one cycle is highlighted in Fig. 1b. The local density around this grain and its velocity are plotted in Fig. 2b-c. Its neighborhood experiences periodic compression and dilation. The velocity of the grain,  $v_g$ , follows the same periodic pattern and shows a positive correlation with  $\phi_{loc}$ , *i.e.*, grains in denser regions tend to move faster. Figure 3 shows the velocity of the particle as a function of  $\phi_{loc}$  averaged over the region of interest and time. For the experiment in Fig. 2 ( $A = 11\text{mm}$ )  $\bar{v}_g$  saturates for low and high  $\phi_{loc}$ , but increases steeply between  $\phi_{loc} = 0.6$  and  $\phi_{loc} = 0.8$ . Note that a similar dependence of  $\bar{v}_g$  on  $\phi_{loc}$  already appears for lower oscillation amplitude ( $A < 11\text{mm}$ ), where no clustering/density wave is observed. Henceforth  $\bar{v}_g$  is referred to as the *presumed velocity* of grains.

The dependence of  $\bar{v}_g$  on  $\phi_{loc}$  reveals the mechanism leading to the clustering. Considering the continuity equation:

$$\frac{\partial \phi_{loc}}{\partial t} + \nabla \cdot (\phi_{loc} \vec{v}) = 0, \quad (1)$$

it is readily to show that an increasing function  $\vec{v}(\phi_{loc})$  would promote the formation of shock waves of  $\phi_{loc}$ . However, the density wave is only observed for  $A \geq 11\text{mm}$ , which suggests that the collisions between grains introduce an equivalent term of pressure and competes with the promotion of  $\vec{v}(\phi_{loc})$ . Therefore, the equation for the velocity field can be written as

$$\frac{\partial \vec{v}}{\partial t} + \vec{v} \cdot \nabla \vec{v} = \frac{\vec{V}_g(\phi_{loc}) - \vec{v}}{\tau} - \frac{1}{\phi_{loc}} \nabla p(\phi_{loc}). \quad (2)$$

The first term at the right hand side is the tendency of the local velocity to match the presumed velocity,  $\vec{V}_g$ , where  $\tau$  is the time scale of the relaxation of  $\vec{v}$  towards  $\vec{V}_g$ . The second term represents the gradient of the pressure arising from the collisions between grains,  $p$ . Note that both  $\vec{V}_g$  and  $p$  are functions of  $\phi_{loc}$ . The presumed velocity,  $\vec{V}_g$ , largely follows the direction of the oscillation. It can be seen in Fig. 2(c) that  $\tau$  is much smaller than the oscillation period. Therefore, we only consider the flow in the oscillation direction, and Eq. 2 is reduced to a scalar equation.

The model embodied in Eqs. 1 and 2 admits a steady-state solution representing the uniform flow ( $\phi_{loc} = \phi_0$  and  $v = V_g(\phi_0)$ ). Nevertheless, such a homogeneous flow is stable against density perturbations, provided

$$(\phi_{loc}V'_g)^2 < p'. \quad (3)$$

$V'_g$  and  $p'$  are the derivatives of  $V_g$  and  $p$  with respect to  $\phi_{loc}$ . If condition 3 is violated, the density disturbance grows and travels at a higher velocity than  $V_g(\phi_0)$  corresponding to homogeneous flow [27]. We use the measured  $\bar{v}_g$  for  $V_g$ . Error function is fitted on the data, thus, the derivative,  $\bar{v}'_g$ , has Gaussian-like peaks. The pressure from collisions is estimated by

$$p = c_0 \bar{\delta v}_g^2 \frac{d_g^2}{\bar{d}(\bar{d} - d^*)} = c_0 \bar{\delta v}_g^2 f(\phi_{loc}). \quad (4)$$

with  $c_0 \approx 2$  (see SI). Its value is later determined by comparing with the experimental observation. For individual grains, the velocity fluctuation  $\delta v_g$  in its neighborhood is extracted. Similar to  $\bar{v}_g$ ,  $\bar{\delta v}_g^2(\phi_{loc})$  is the average of  $\delta v_g^2$  over the region of interest and time for a given  $\phi_{loc}$ .  $\bar{d} = d_g/\sqrt{\phi_{loc}}$  represents the average distance between grains for a given  $\phi_{loc}$ , and  $d^* = d_g/\sqrt{\phi^*}$  corresponds to the hexagonal packing. The fraction on the right hand side of Eq. 4 is purely geometrical and is referred to as  $f(\phi_{loc})$  in the following.  $f(\phi_{loc})$  increases with  $\phi_{loc}$  and diverges when approaching  $\phi_{loc} = \phi^*$ . In contrast, though increasing with  $A$ ,  $\bar{\delta v}_g^2$  is largely constant for a given  $A$  (refer to SI). Therefore, the variant of  $p$  is dominated by  $f(\phi_{loc})$ , and its derivative is approximated by  $p' \approx c_0 \bar{\delta v}_g^2 f'(\phi_{loc})$ .

Figure 4 illustrates the condition Eq. 3. The packing density in the region of interest for  $A < 11\text{mm}$  is indicated by a gray bar ( $\phi_0 \in [0.61, 0.62]$ ). Because particles moves slower than the container/side wall, there is always an empty area not containing grains. This empty area can be seen in Fig. 1a and more salient on the right side of the container in Fig. 1b. Therefore,  $\phi_0$  is proportional but larger than  $\phi_{tot}$  in general.  $c_0 = 1.8$  is chosen such

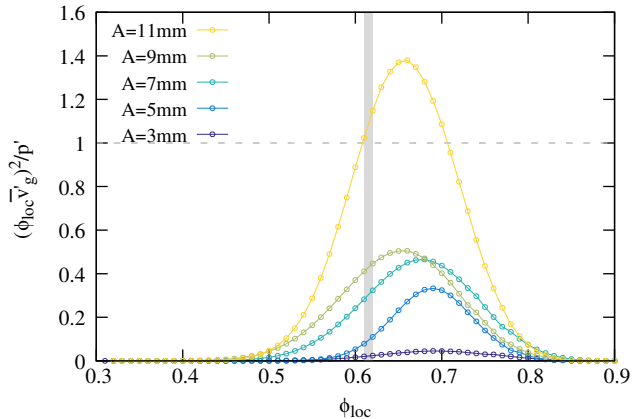


FIG. 4. The ratio of the two terms in Eq. 3 are plotted. The region where the ratio is larger than 1 indicates the violation of Eq. 3. The vertical gray bar indicates the density in the region of interest,  $\phi_0$ , for the oscillation amplitude without clustering.

that Eq. 3 is just violated for  $A = 11\text{mm}$  at  $\phi_0$ , but not for smaller oscillation amplitude. Though both  $p'$  (or  $\delta v_g^2$ ) and  $\bar{v}_g'$  increase with the oscillation strength, the relative increase of the latter is more significant. In consequence, the instability is triggered by increasing  $A$  beyond the transition amplitude,  $A_c$ . This corresponds to the observed ‘freezing by heating’.

Figure 4 provides further insight. The instability associated with the violation of Eq. 3 would only be initialized for packings of intermediate densities, where the ratio  $(\phi_{loc}\bar{v}_g')^2/p'$  displays a peak. The peak shape leads to the a non-monotonic dependence of the transition amplitude,  $A_c$ , on the global packing density of the system,  $\phi_{tot}$ . Imagine that  $\phi_{tot}$  is increased from 0.505 (analyzed so far) towards  $\phi^*$ . Before reaching the peak of  $(\phi_{loc}\bar{v}_g')^2/p'$  the transition amplitude,  $A_c$ , would reduce. However, it would raise quickly again when  $\phi_{tot}$  is increased beyond the peak.  $p'$  diverges at  $\phi^*$ , and so does  $A_c$ .

The above hypothesis is examined in experiments. The function  $A_c(\phi_{tot})$  is plotted in Fig. 5. The lowest density where spontaneous clustering is observed is  $\phi_{tot} \approx 0.505$ . The minimum of  $A_c$  is reached for  $\phi_{tot} \approx 0.64$ . The shape of the function  $A_c(\phi_{tot})$  is in agreement with the model. However, the dip of  $A_c$  close to the crystalline density ( $\phi_{tot} \approx 0.9$ ) is not expected in the model, since the divergence of  $p$  is supposed to suppress any density wave formation. In practice, when the pressure rising from the collision between grains exceeds that resulting from gravity, grains jump over each other, and the 2D packing scenario used so far breaks down. For dense packings ( $\phi_{tot} \gtrsim 0.7$ ) we observed such behavior near the wall,

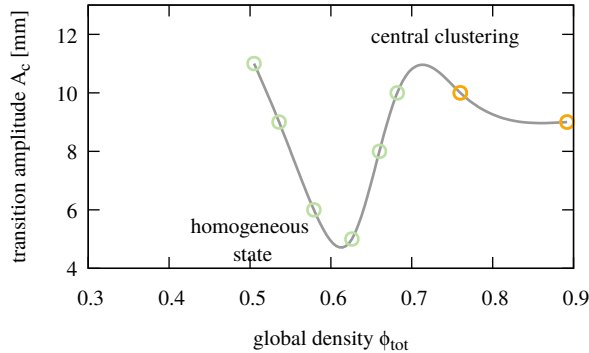


FIG. 5. The transition amplitude,  $A_c$ , triggering the clustering is a non-monotonic function of the global packing density  $\phi_{tot}$ . The lowest  $\phi_{tot}$  of the spontaneous clustering is 0.51 for the tested range of  $A$ . The last two points where the 2D packing scenario breaks down are highlighted by orange. The solid line serves as guide for the eye.

and the packing density at the center is decreased, which allows the formation of clusters.

We have elaborated the mechanism of clustering by the instability analysis of the uniform flow in a phenomenological model (Eqs. 1 and 2). The key ingredient promoting the clustering is the dependence of the presumed velocity of grains on the the local density. Why does such a dependence exist? We believe that it is a consequence of the interplay between the friction between grains and that between grains and the substrate.  $\mu_{gg}$  and  $\mu_{gs}$  denote the friction coefficients of the former and the latter respectively, and  $F_{gg}$  and  $F_{gs}$  are the corresponding friction forces. Upon agitation  $F_{gs}$  accelerates not only the linear momentum but also the angular momentum of individual grains. It has been shown that the rotational degree of freedom effectively reduces the maximum velocity that individual grains could reach by the action of  $F_{gs}$  alone [26]. The faster a grain rolls, the slower its linear velocity [20]. Consider now the collision of two grains rolling in the same direction. Then  $F_{gg}$  counteracts the rolling of grains which in turn increases the moment of the inertia with respect to  $F_{gs}$  and effectively enhances the linear momentum transfer.  $F_{gg}$  is proportional to  $p$ , and  $p$  increases with  $\phi_{loc}$  and  $A$ . Therefore, grains tend to move faster in dense areas and/or under stronger agitations. These arguments lead to the features of the function  $v_g(\phi_{loc}, A)$  shown in Fig. 3, where  $v_g$  increases with both  $\phi_{loc}$  and  $A$ . In order to further support this line of arguments DEM simulations are performed using LIGGGHTS [28]. For a given  $\mu_{gs}$  and  $A$ , the clustering is suppressed by decreasing  $\mu_{gg}$ . See SI for more information.

The clustering phenomenon reported here could be reproduced in experiments with poly-disperse grains of diameter 0.8-1 mm, various surface types (smooth and rough glass beads), aspheric grains (e.g., millet seeds) and in a square container. Therefore, the principle of clustering is robust for the explored parameter range. A complete quantitative understanding of the clustering, its growth/coarsening and the potential relation to segregation [21] requires further work. In particular, we notice that the presumed velocity includes certain non-local effect, as in the dense phase correlations between velocities of individual particles develop. This non-local effect increases with  $\phi_{tot}$  and promotes the significant increase of  $\bar{v}'_g$  near  $A_c$ . An appropriate hydrodynamic treatment of this term is anticipated in the future research.

This work is supported by German Science Foundation.

- 
- [1] Schnautz, T., Brito, R., Kruehle, C. A. & Rehberg, I. A Horizontal Brazil-Nut Effect and Its Reverse. *Phys. Rev. Lett.* **95** (2005).
  - [2] Goldhirsch, I. Rapid granular flows. *Annu. Rev. Fluid Mech.* **35**, 267–293 (2003).
  - [3] Herminghaus, S. & Mazza, M. G. Phase separation in driven granular gases: exploring the elusive character of nonequilibrium steady states. *Soft Matter* **13**, 898–910 (2017).
  - [4] Goldhirsch, I. & Zanetti, G. Clustering instability in dissipative gases. *Phys. Rev. Lett.* **70**, 1619–1622 (1993).
  - [5] Umbanhowar, P. B., Melo, F. & Swinney, H. L. Localized excitations in a vertically vibrated granular layer. *Nature* **382**, 793 (1996).
  - [6] Krenzel, D., Strobl, S., Sack, A., Heckel, M. & Pöschel, T. Pattern formation in a horizontally shaken granular submonolayer. *Granular Matter* **15**, 377–387 (2013).
  - [7] Aumaître, S., Schnautz, T., Kruehle, C. A. & Rehberg, I. Granular Phase Transition as a Precondition for Segregation. *Phys. Rev. Lett.* **90** (2003).
  - [8] Cafiero, R., Luding, S. & Herrmann, H. J. Two-Dimensional Granular Gas of Inelastic Spheres with Multiplicative Driving. *Phys. Rev. Lett.* **84**, 6014–6017 (2000).
  - [9] Hummel, M. *Hydrodynamics of granular gases: Clustering, universality and importance of subsonic convective waves*. Ph.D. thesis, Georg-August-Universität, Göttingen (2016).
  - [10] Aranson, I. S. & Tsimring, L. S. Patterns and collective behavior in granular media: Theo-

- retical concepts. *Rev. Mod. Phys.* **78**, 641–692 (2006).
- [11] Olafsen, J. S. & Urbach, J. S. Clustering, Order, and Collapse in a Driven Granular Monolayer. *Phys. Rev. Lett.* **81**, 4369–4372 (1998).
- [12] Kondic, L. Dynamics of spherical particles on a surface: Collision-induced sliding and other effects. *Phys. Rev. E* **60**, 751–770 (1999).
- [13] Kurtze, D. A. & Hong, D. C. Traffic jams, granular flow, and soliton selection. *Phys. Rev. E* **52**, 218 (1995).
- [14] Kloss, C., Goniva, C., Hager, A., Amberger, S. & Pirker, S. Models, algorithms and validation for opensource dem and cfd-dem. *Progress in Computational Fluid Dynamics, An Int. J.* **12**, 140–152 (2012).
- [15] Schnautz, T., Brito, R., Kruehle, C. A. & Rehberg, I. A Horizontal Brazil-Nut Effect and Its Reverse. *Phys. Rev. Lett.* **95** (2005).
- [16] Goldhirsch, I. Rapid granular flows. *Annu. Rev. Fluid Mech.* **35**, 267–293 (2003).
- [17] Herminghaus, S. & Mazza, M. G. Phase separation in driven granular gases: exploring the elusive character of nonequilibrium steady states. *Soft Matter* **13**, 898–910 (2017).
- [18] Goldhirsch, I. & Zanetti, G. Clustering instability in dissipative gases. *Phys. Rev. Lett.* **70**, 1619–1622 (1993).
- [19] Umbanhowar, P. B., Melo, F. & Swinney, H. L. Localized excitations in a vertically vibrated granular layer. *Nature* **382**, 793 (1996).
- [20] Krenkel, D., Strobl, S., Sack, A., Heckel, M. & Pöschel, T. Pattern formation in a horizontally shaken granular submonolayer. *Granular Matter* **15**, 377–387 (2013).
- [21] Aumaître, S., Schnautz, T., Kruehle, C. A. & Rehberg, I. Granular Phase Transition as a Precondition for Segregation. *Phys. Rev. Lett.* **90** (2003).
- [22] Cafiero, R., Luding, S. & Herrmann, H. J. Two-Dimensional Granular Gas of Inelastic Spheres with Multiplicative Driving. *Phys. Rev. Lett.* **84**, 6014–6017 (2000).
- [23] Hummel, M. *Hydrodynamics of granular gases: Clustering, universality and importance of subsonic convective waves*. Ph.D. thesis, Georg-August-Universität, Göttingen (2016).
- [24] Aranson, I. S. & Tsimring, L. S. Patterns and collective behavior in granular media: Theoretical concepts. *Rev. Mod. Phys.* **78**, 641–692 (2006).
- [25] Olafsen, J. S. & Urbach, J. S. Clustering, Order, and Collapse in a Driven Granular Monolayer. *Phys. Rev. Lett.* **81**, 4369–4372 (1998).

- [26] Kondic, L. Dynamics of spherical particles on a surface: Collision-induced sliding and other effects. *Phys. Rev. E* **60**, 751–770 (1999).
- [27] Kurtze, D. A. & Hong, D. C. Traffic jams, granular flow, and soliton selection. *Phys. Rev. E* **52**, 218 (1995).
- [28] Kloss, C., Goniva, C., Hager, A., Amberger, S. & Pirker, S. Models, algorithms and validation for opensource dem and cfd–dem. *Progress in Computational Fluid Dynamics, An Int. J.* **12**, 140–152 (2012).